Received: 30 March 2022 | Revised: 31 May 2022 | Accepted: 15 June 2022

DOI: 10.1111/mpp.13246

Molecular Plant Pathology WILEY

ORIGINAL ARTICLE

Barley guanine nucleotide exchange factor *Hv*GEF14 is an activator of the susceptibility factor *Hv*RACB and supports host cell entry by *Blumeria graminis* f. sp. *hordei*

Adriana Trutzenberg | Stefan Engelhardt | Lukas Weiß | Ralph Hückelhoven

Chair of Phytopathology, School of Life Sciences, Technical University of Munich, Freising-Weihenstephan, Germany

Correspondence
Ralph Hückelhoven, Chair of Phytopathology, School of Life Sciences, Technische Universität München, Emil-Ramann-Str. 2, D-85354 Freising, Munich, Germany.
Email: hueckelhoven@tum.de

Funding information
Deutsche Forschungsgemeinschaft, Grant/Award Number: SFB924

Abstract

In barley (*Hordeum vulgare*), signalling rat sarcoma homolog (RHO) of plants guanosine triphosphate hydrolases (ROP GTPases) support the penetration success of *Blumeria graminis* f. sp. *hordei* but little is known about ROP activation. Guanine nucleotide exchange factors (GEFs) facilitate the exchange of ROP-bound GDP for GTP and thereby turn ROPs into a signalling-activated ROP-GTP state. Plants possess a unique class of GEFs harbouring a plant-specific ROP nucleotide exchanger domain (PRONE). Here, we performed phylogenetic analyses and annotated barley PRONE-GEFs. The leaf epidermal-expressed PRONE-GEF *HvGEF14* undergoes a transcriptional down-regulation on inoculation with *B. graminis* f. sp. *hordei* and directly interacts with the ROP GTPase and susceptibility factor *Hv*RACB in yeast and in planta. Overexpression of activated *Hv*RACB or of *Hv*GEF14 led to the recruitment of ROP downstream interactor *Hv*RIC171 to the cell periphery. *Hv*GEF14 further supported direct interaction of *Hv*RACB with a *Hv*RACB-GTP-binding CRIB (Cdc42/Rac Interactive Binding motif) domain-containing *Hv*RIC171 truncation. Finally, the overexpression of *HvGEF14* caused enhanced susceptibility to fungal entry, while *HvGEF14* RNAi provoked a trend to more penetration resistance. *Hv*GEF14 might therefore play a role in the activation of *Hv*RACB in barley epidermal cells during fungal penetration.

KEYWORDS
barley, epidermis, fluorescence lifetime imaging, penetration resistance, plant-specific ROP nucleotide exchanger, powdery mildew, RHO of plants

1 | INTRODUCTION

ROPs (rat sarcoma homolog [RHO] of plants) are small monomeric GTPases that function as signalling hubs in cell polarity processes that involve cytoskeleton reorganization (Mucha et al., 2011). Pollen tube growth, the development of epidermal pavement cells and root hairs, but also processes that are important during plant–microbe interactions are examples of ROP-regulated processes (Engelhardt et al., 2020; Zheng & Yang, 2000). ROPs are considered molecular switches due to their ability to shuttle between a signalling-inactive, guanosine diphosphate (GDP)-bound state and a signalling-activated guanosine triphosphate (GTP)-bound state (Bloch & Yalovsky, 2013). An interaction with downstream signalling partners, and therefore signal transduction, only occurs in the GTP-bound state (Nagawa

et al., 2010). To locally interact with downstream signalling partners, ROPs further require to be membrane-associated, which is achieved by posttranslational lipid modifications and electrostatic lipid interaction (Winge et al., 2000; Yalovsky, 2015).

Barley (*Hordeum vulgare* [*Hv*]) contains six ROPs: *Hv*RACB, *Hv*RACD, *Hv*RAC1, *Hv*RAC3, *Hv*ROP4, and *Hv*ROP6 (Schultheiss et al., 2003). Studies using barley plants overexpressing constitutively activated (CA) variants of *Hv*RACB, *Hv*RAC1, or *Hv*RAC3 indicated a role for these ROPs in plant development. Additionally, these plants support either enhanced or reduced susceptibility to penetration by fungal leaf pathogens such as *Blumeria graminis* f. sp. *hordei* (Bgh) and the rice blast fungus *Magnaporthe oryzae* (Pathuri et al., 2008; Schultheiss et al., 2005). *Hv*RACB in particular has been studied for its function in susceptibility to penetration and accommodation of haustoria from Bgh. In addition, a function of *Hv*RACB in polar epidermal cell development has been shown. *Hv*RACB is hence considered a key developmental protein that is co-opted by Bgh during pathogenesis (Engelhardt et al., 2020).

Due to the vast number of signalling processes ROPs are involved in, it is apparent that a tight regulation of these molecular switches is required to fine-tune the cellular mechanisms following ROP activation. This regulation is controlled by three classes of regulatory proteins: guanine nucleotide exchange factors (GEF), GTPase activating proteins (GAP), and guanine nucleotide dissociation inhibitors (GDI) (Nagawa et al., 2010; Vetter & Wittinghofer, 2001; Zheng & Yang, 2000). Regarding ROP signalling, GEFs are ROP-signalling activating proteins that interact with ROPs to induce a conformational change facilitating the exchange of GDP by GTP (Berken et al., 2005; Thomas et al., 2007, 2009).

Plants evolved a specific class of GEFs with a highly conserved plant-specific Rac/ROP nucleotide exchanger (PRONE) domain (Berken et al., 2005; Gu et al., 2006). The family of PRONE-GEFs in the model plant *Arabidopsis thaliana* consists of 14 members that have been studied for their function in various polar growth processes, plant development (Chang et al., 2013; Chen et al., 2011; Gu et al., 2006; Huang et al., 2018), and immunity (Qu et al., 2017). So far, the PRONE domain is the only identified conserved part of these GEFs. It contains several interfaces that physically interact with ROPs in a heterotetrameric complex of two ROPs with two PRONE-GEFs. After binding to ROPs, the PRONE domain facilitates a structural rearrangement, which leads to GDP release. Nucleotide-free ROPs and GEFs can further interact as a stable complex (Berken et al., 2005; Chang et al., 2013; Gu et al., 2006; Thomas et al., 2007). The PRONE domain is flanked by N- and C-terminal variable regions that probably possess regulatory functions. The C-terminal stretch can be subject to phosphorylation by upstream receptor-like kinases (RLK) that have been implicated in developmental as well as immunity-related signalling pathways (Fehér & Lajkó, 2015). One example of RLK-GEF-ROP signalling involves the RLK FERONIA, which interacts directly with *At*GEF14 in *A. thaliana*. Further downstream, *At*GEF14 interacts with *At*ROP6, which functions in the polar growth of epidermal cells (Lin et al., 2022) and together with *At*RIC1 facilitates microtubule organization to deal with mechanical stress (Tang et al., 2022). Furthermore, *At*GEF14 localizes to the apical region of pollen tubes and interacts with *At*ROP1, a regulator of pollen tube growth (Gu et al., 2006). In roots, *At*GEF14 may be also involved in polar growth processes. *At*GEF14 accumulates at the root hair initiation site and is replaced by other GEFs during the root hair initiation and elongation phase (Denninger et al., 2019). We know little about the function of PRONE-GEFs in the interaction of plants with fungal pathogens. In rice, *Os*GEF1 interacts with the RLK *Os*CERK1, a central part of the rice chitin receptor complex, and activates *Os*RAC1 for its function in defence against *M. oryzae* (Akamatsu et al., 2013).

Susceptibility factors, such as the ROP GTPase *Hv*RACB, have become increasingly recognized as potential targets for breeding but often little is known about their mode of activation and corresponding molecular environment. This work investigates barley PRONE-GEFs, focusing on *Hv*GEF14 as an interactor of *Hv*RACB. We report that *Hv*GEF14 is expressed in the leaf epidermis and downregulated after inoculation with Bgh. *Hv*GEF14 can bind to *Hv*RACB in yeast and in planta, and may be involved in the activation of this susceptibility-associated barley ROP in leaf epidermal cells.

2 | RESULTS

2.1 | Phylogenetic analysis reveals three distinct clades of barley PRONE-GEFs

To investigate GEFs in barley, we concentrated on the PRONE domain-containing class of exchange factors (Berken et al., 2005). We identified 11 PRONE domain-encoding genes in *H. vulgare* 'Morex' genome version 3 (Mascher et al., 2021) and aligned full-length primary amino acid sequences of all barley PRONE-GEFs with 11 PRONE-GEFs of *Oryza sativa* and 14 PRONE-GEFs of *A. thaliana*. Because the *O. sativa* PRONE-GEF annotation has been incomplete so far, we first constructed a maximum-likelihood phylogenetic tree in which all *O. sativa* PRONE-GEFs were annotated according to their primary sequence similarity to *A. thaliana* PRONE-GEFs using the nomenclature by Berken et al. (2005) (Figure S1). Subsequently, another calculation was performed to obtain the phylogenetic tree with all three species (Figure 1, based on the MUSCLE alignment in Figure S2). *H. vulgare* PRONE-GEFs were then annotated according to the closely related *O. sativa* PRONE-GEFs to determine a nomenclature that is consistent for grasses. In this way, the 11 barley PRONE-GEFs were named *Hv*GEFs 1, 3a, 3b, 3c, 7a, 7b, 9a, 9b, 9c, 10, and 14. The phylogenetic tree shows three distinct clades, with clade III containing only PRONE-GEF14 proteins from all three species (Figure 1). Notably, in clades I and II, PRONE-GEFs from monocot species show plant clade-specific clustering with high confidence. This suggests lineage-specific proliferation of PRONE-GEF genes after the separation of monocots from dicots.

The three PRONE-GEF14 sequences differ not only in their N- and C-terminal regions from the other PRONE-GEFs but present higher levels of amino acid variations in the PRONE domain itself when compared to all other PRONE-GEFs (Figures S1 and S2, and Table S1).

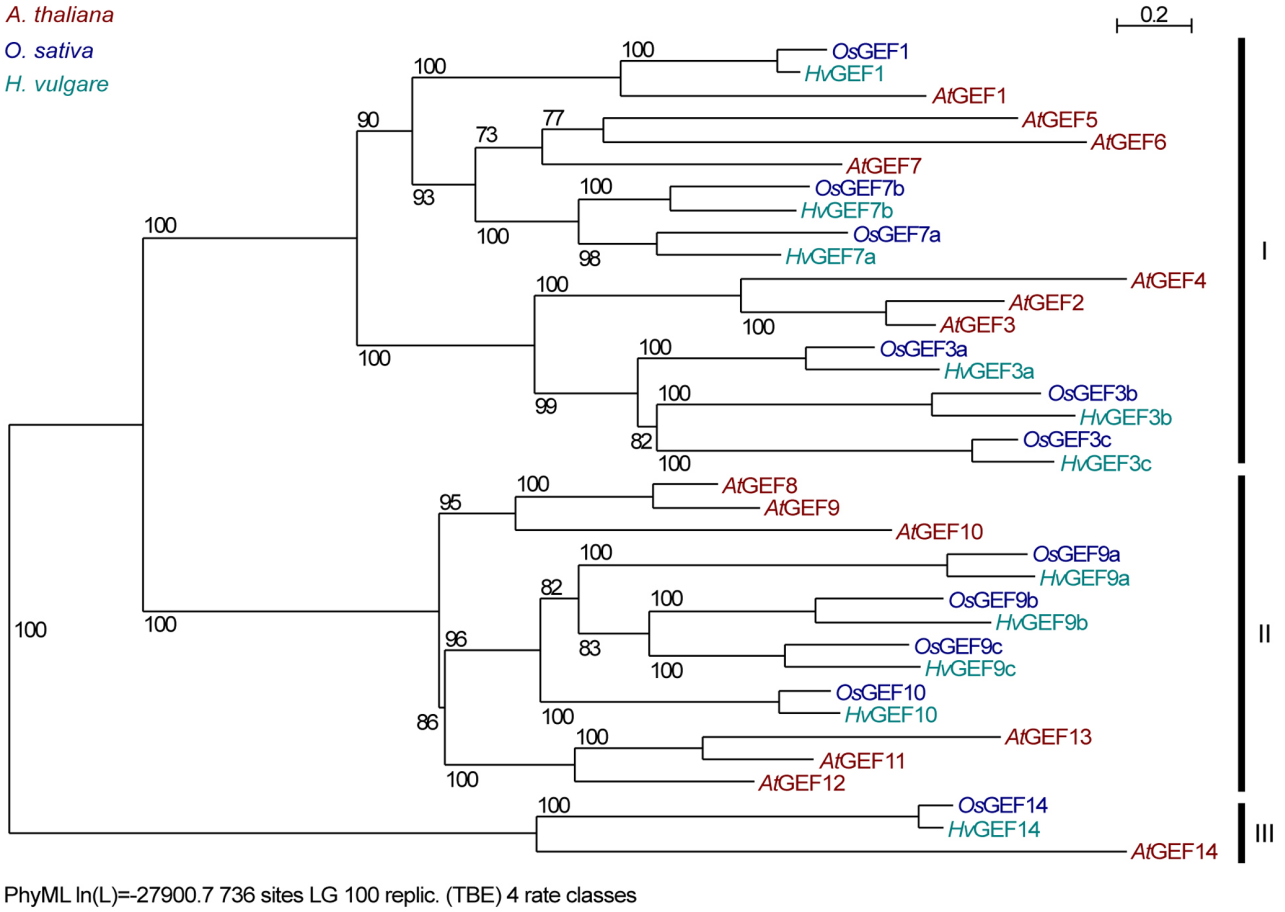

FIGURE 1 PRONE-GEFs cluster in three distinctive clades. Phylogenetic analysis of PRONE-GEFs of *Arabidopsis thaliana* (At), *Oryza sativa* (Os), and *Hordeum vulgare* (Hv) based on MUSCLE alignment. The maximum-likelihood tree was calculated based on available amino acid sequences (NCBI and barley Morex genome version 3) and annotation of barley PRONE-GEFs was performed based on this tree.

Despite its unique position in the phylogenetic tree, the overall design of the *Hv*GEF14 PRONE domain is conserved with its three subdomains (Figure 2). The alignment of the 11 barley PRONE-GEFs highlights the predicted PRONE domains with varying length of 344 amino acids (*Hv*GEF10) to 379 amino acids (*Hv*GEF3a) (Figure S1 and Table S2). *Hv*GEF3a has no variable C-terminal region beyond the PRONE domain, and the C-termini of *Hv*GEF3b and *Hv*GEF3c are comparably short (Figures 2 and S1, and Table S2). *Hv*GEF9a is predicted to contain only a short variable N-terminus of 43 amino acids. It is evident from the alignment that, regarding the primary sequence, *Hv*GEF14 substantially differs most from all other barley PRONE-GEFs. In addition, the variability in the primary sequence of *Hv*GEF14 is highest when compared to the consensus sequence of all 11 *Hv*-GEFs (Figure S1 and Table S1). However, important residues for GEF-GEF homodimerization (Thomas et al., 2007), such as phenylalanine 133 and leucine 138 (in *Hv*GEF14), are conserved and we found that *Hv*GEF14 interacted with itself or its PRONE domain in yeast two-hybrid (Y2H) assays (Figure S3). Known residues involved in GEF-ROP interaction (N161, Q206, E215, M217, W275, W276, L434, and R460; Thomas et al., 2007) are also conserved in *Hv*GEF14. Furthermore, serine 394 in the *Hv*GEF14 PRONE domain is a predicted phosphorylation site based on mass spectrometry analysis of phosphorylation sites in *A. thaliana* GEF14 (Mergner et al., 2020) (Figure 2).

2.2 | *Hv*GEF14 is expressed in epidermal cells and downregulated after Bgh inoculation

To understand the potential function of barley PRONE-GEFs, gene expression patterns in different tissues were investigated. An initial in silico expression analysis of the eight barley *PRONE-GEFs* was performed by consulting the RNA sequencing (RNA-Seq) database provided by the James Hutton Institute (https://ics.hutton.ac.uk/barleyGenes). The data show RNA fragments per reads per kilobase million (FPKM) of the barley *PRONE-GEFs* in distinct tissues. *HvGEF3a*, for example, is mainly expressed in the developing embryo. Other barley *GEFs*, such as *HvGEF1*, show a broader expression pattern, with the highest number of RNA fragments detected in embryos, root, and grains. *HvGEF14* is the most ubiquitously expressed barley *PRONE-GEF*, with the highest fragment counts in almost all tissues except in senescing leaves. Interestingly, *HvGEF1* and *HvGEF14* are the only GEF genes expressed in seedling shoots and epidermal peels, with *HvGEF14* showing the highest fragment counts in these two tissues (Table S3). The leaf

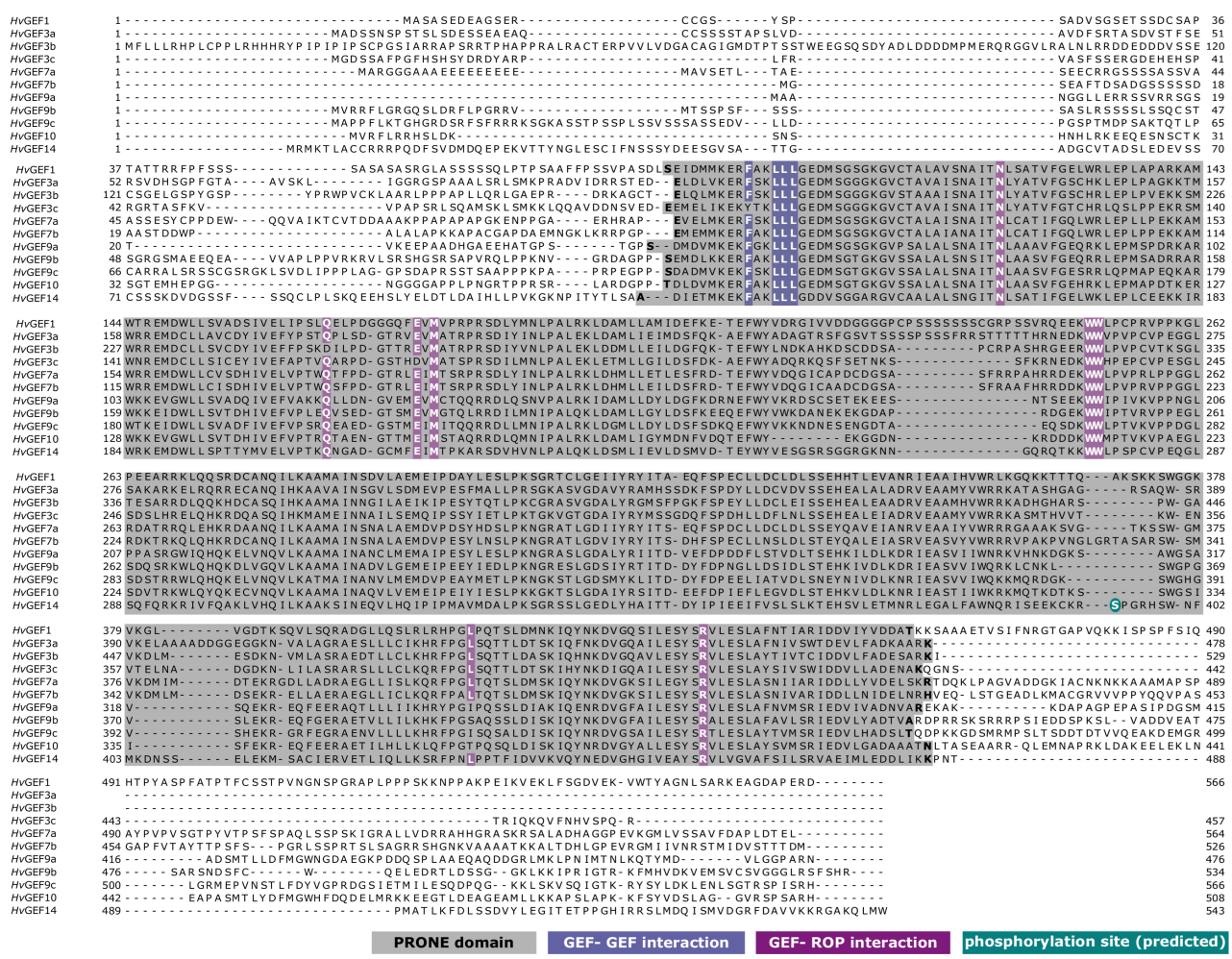

FIGURE 2 *Hordeum vulgare* (*Hv*) PRONE-GEF MUSCLE alignment with annotation of PRONE domain (according to NCBI prediction) in grey, and GEF–GEF interaction residues and ROP–GEF interaction residues highlighted in purple. Predicted phosphorylation site in *Hv*GEF14 highlighted in turquoise. Protein IDs according to NCBI accessions and annotation based on MUSCLE alignment with *Oryza sativa* PRONE-GEFs (see Figure S1).

epidermis of barley provides an important interface for plant–pathogen interaction. Because the barley ROP *Hv*RACB has been shown to play a crucial role in epidermis development and susceptibility to Bgh, we concentrated on PRONE-GEFs, which might be of importance to signal transduction in the epidermis. We confirmed the gene expression of *HvGEF14* via reverse transcription-quantitative PCR (RT-qPCR) in leaf and leaf epidermis from 7-day-old leaves of the barley cultivar Golden Promise. In three independent biological replicates, we found higher transcript levels of *HvGEF14* in the epidermis when compared to whole leaves (Figure 3a). Notably, in three independent biological experiments, the *HvGEF14* expression level in the epidermis decreased after inoculation with the biotrophic powdery mildew fungus Bgh compared to epidermal peels from unchallenged leaves (Figure 3b).

2.3 | *Hv*GEF14 interacts with *Hv*RACB

So far, nothing is known about potential PRONE-GEF-mediated activation of barley ROPs. To check if *Hv*GEF14 could function as an *Hv*RACB-activating PRONE-GEF, we analysed the direct protein–protein interaction between *Hv*RACB and *Hv*GEF14 in yeast and in planta. Plant ROPs can be mutagenized in the GTPase domain (e.g., *Hv*RACB-G15V) to render the ROP constitutively activated (CA) (Schultheiss et al., 2003). Correspondingly, the *Hv*RACB-T20N substitution results in a dominant negative (DN), signalling-inactive conformation. A third mutation (*Hv*RACB-D121N) leads to lower nucleotide affinity and potentially increases GEF-binding affinity (Akamatsu et al., 2013; Berken et al., 2005; Cool et al., 1999). Interestingly, we found that full-length *Hv*GEF14 and the *Hv*GEF14 PRONE domain (amino acids 124–485) directly interacted in yeast with wild-type (WT) *Hv*RACB, CA *Hv*RACB-G15V, and the low nucleotide affinity version *Hv*RACB-D121N, but not with the DN *Hv*RACB-T20N variant (Figure 4a, see also Figure S4 for the full drop-out plates). All *Hv*RACB variants were truncated at the *Hv*RACB CSIL motif to inhibit prenylation and membrane association in yeast and hence facilitate protein accumulation in yeast nuclei. To substantiate the results, we performed western blotting, which confirmed protein stability in yeast (Figure S5). In addition, similar

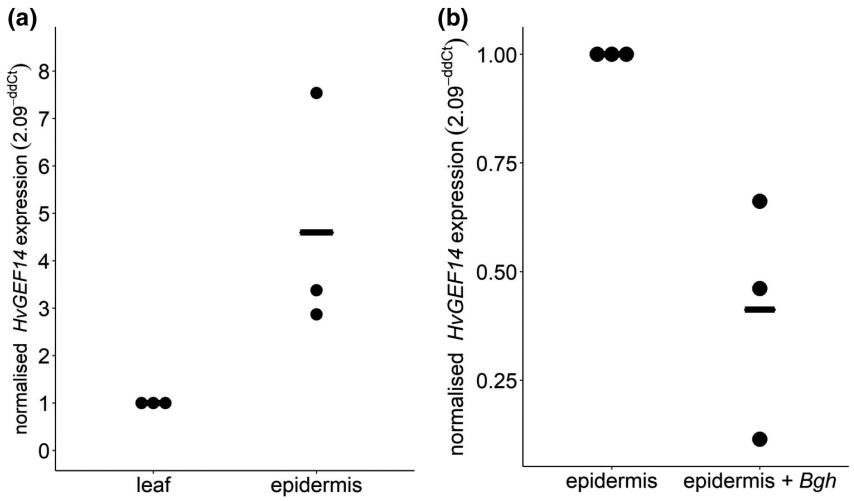

FIGURE 3 *HvGEF14* shows increased expression in epidermal peels and downregulation after inoculation with fungal spores. *HvGEF14* is expressed in barley epidermis (a) and downregulated after Bgh inoculation (1 day postinoculation) (b) in three independent repetitions (plants harvested on different days). Foldchange expression was calculated with primer efficiency correction and the $2^{-\Delta\Delta Ct}$ method by Livak and Schmittgen (2001) and normalized to transcript levels in whole leaves (a) and noninoculated epidermis (b).

results were obtained in Y2H assays using the type II ROP *Hv*RAC1 (Figures S6 and S7).

To test direct protein–protein interaction between *Hv*GEF14 and *Hv*RACB in planta, we measured Förster resonance energy transfer by fluorescence lifetime imaging (FRET-FLIM) in transiently transformed barley epidermal cells (Figure 4b,c). The monomeric enhanced green fluorescent protein (eGFP) fusion meGFP-*Hv*GEF14 served as a FRET-donor and was used as a potential interaction partner in all combinations tested. As FRET acceptor, different variants of mCherry-*Hv*RACB (WT, G15V, D121N, T20N) and cytosolic mCherry were used. All measurements took place at the cell periphery at the equatorial cell plane (Figure 4b).

meGFP-*Hv*GEF14 showed a significant lifetime reduction in epidermal cells when transiently co-expressed with mCherry-*Hv*RACB WT to 2.36 ns on average compared to the negative control (free mCherry) recorded at 2.57 ns. This shows that *Hv*GEF14 interacts directly with WT *Hv*RACB in planta (Figure 4c). The transient co-expression of meGFP-*Hv*GEF14 with mCherry-CA *Hv*RACB-G15V also resulted in a significantly reduced GFP-lifetime of 2.32 ns on average. This reflects the interaction assays in yeast and provides further evidence that *Hv*GEF14 can also interact with the CA variant *Hv*RACB-G15V in planta (Figure 4c). In contrast to that, co-expression of mCherry-*Hv*RACB-D121N moderately decreased the meGFP-*Hv*GEF14 lifetime to 2.45 ns on average, which was not significantly different from the negative control (Figure 4c). As observed in Y2H assays, there was no measurable interaction between *Hv*GEF14 and DN *Hv*RACB-T20N in planta (Figure 4b,c). In total, the FRET-FLIM experiments suggest a direct interaction between *Hv*GEF14 full length and *Hv*RACB WT and CA *Hv*RACB-G15V in planta.

2.4 | *Hv*GEF14 overexpression leads to activation of barley ROPs

ROP interacting proteins often display a change of subcellular localization in the presence of an activated ROP. This change in localization is considered evidence for local ROP activity because those interactors preferably interact with GTP-loaded ROPs (Li et al., 2020; McCollum et al., 2020; Schultheiss et al., 2008). In transiently transformed epidermal cells, CA *Hv*RACB-G15V is partially located at the cell periphery, which depends on its C-terminal CSIL prenylation motif (Schultheiss et al., 2003, 2008). *Hv*RIC171, a barley scaffold protein that directly interacts with CA but not DN barley ROP variants (Schultheiss et al., 2008), was recruited from the cytoplasm to the cell periphery and plasma membrane in the presence of co-expressed CA *Hv*RACB-G15V but not DN *Hv*RACB-T20N (Figure 5c). The plasma membrane recruitment of *Hv*RIC171 is therefore considered to be *Hv*RACB activation-dependent (Schultheiss et al., 2008). Based on this, we monitored the localization of mCherry-*Hv*RIC171 in barley epidermis cells in the presence or absence of co-expressed *Hv*GEF14 to analyse the activation potential of *Hv*GEF14 towards *Hv*ROPs. mCherry-*Hv*RIC171 fluorescence significantly increased at the cell periphery when either CA *Hv*RACB-G15V or *Hv*GEF14 was present compared to the empty vector (EV) or DN *Hv*RACB-T20N controls (Figure 5a–c). This was evident from an increase in normalized fluorescent signal intensity at the cell periphery in the equatorial plane of the cell. Additionally, mCherry-*Hv*RIC171 signals appeared very irregular in the cell periphery of control cells, whereas mCherry-*Hv*RIC171 more evenly labelled the cell periphery in cells co-expressing *Hv*GEF14 (Figure 5a, lower panel).

CRIB (Cdc42/Rac interactive binding motif) domains of RHO-interacting proteins specifically bind to GTP-loaded RHO and ROP proteins, and are therefore often used as RHO activity sensors. To test the specific activation of *Hv*RACB in planta, we used *Hv*CRIB46, which represents a fragment of *Hv*RIC171 containing the CRIB domain and was shown before to interact with CA *Hv*RACB-G15V but not DN *Hv*RACB-T20N (Schultheiss et al., 2008). Based on this, we established a FRET-based activity sensor probe containing N-terminally meGFP-tagged *Hv*RACB and C-terminally mCherry-tagged *Hv*CRIB46 on individual plasmids. To reduce interference of endogenous signalling components in barley, the measurements were performed in *Nicotiana benthamiana*. meGFP-*Hv*RACB WT did not interact with the negative control GST-mCherry (average meGFP lifetime of 2.62 ns), but the meGFP-*Hv*RACB WT lifetime was significantly reduced when meGFP-*Hv*RACB WT was co-expressed with

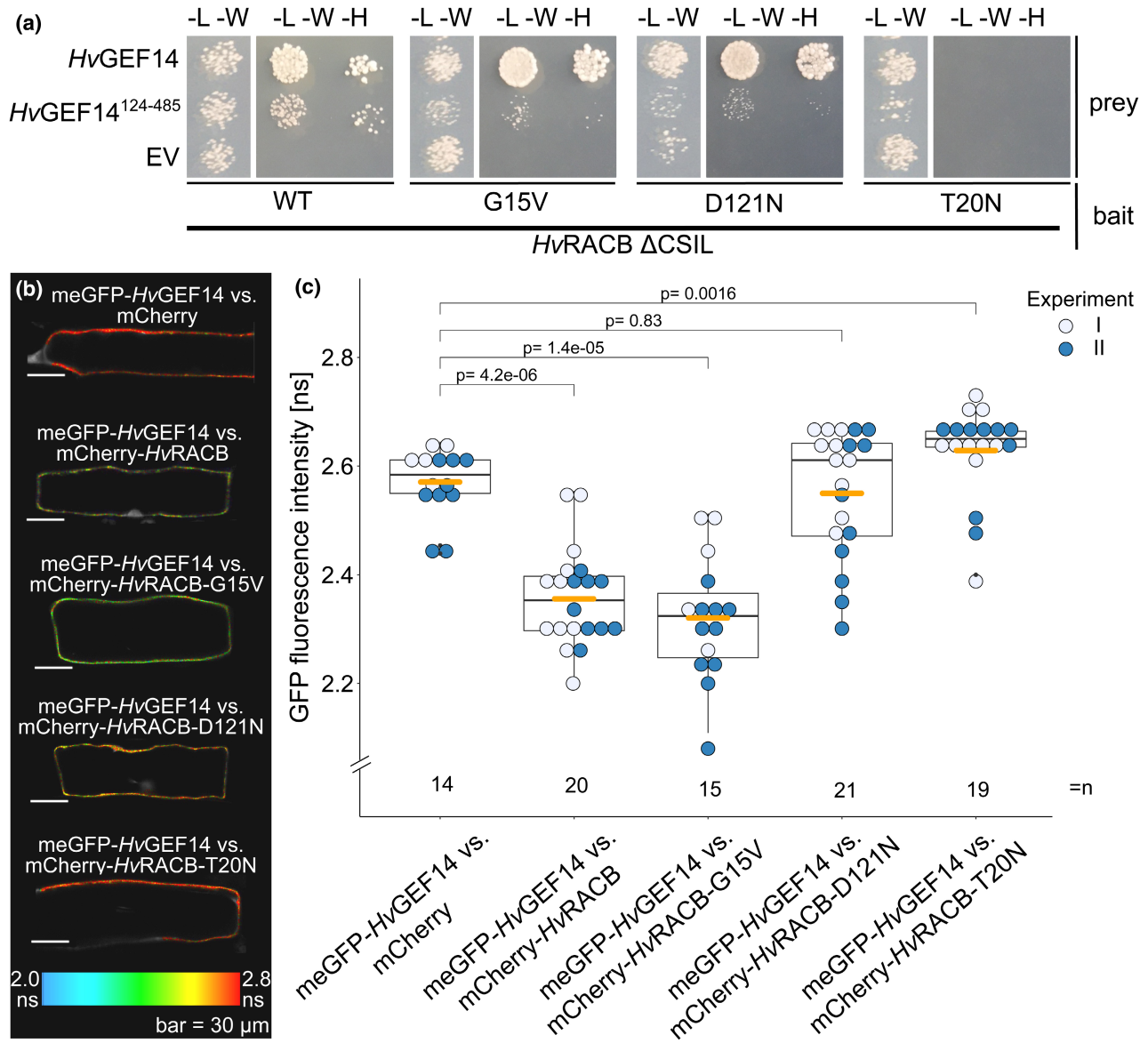

FIGURE 4 *Hv*GEF14 interacts with barley ROP variants in yeast and in planta. (a) *Hv*RACB wild type (WT), G15V constitutively activated (CA), D121N low nucleotide affinity, and T20N dominant negative (DN) variants were tested as bait against prey constructs *Hv*GEF14 full length, *Hv*GEF14 amino acids 124–485 (PRONE domain), or empty vector (EV). Interaction of proteins shown on medium containing amino acid mix without leucine (L), tryptophan (W), and histidine (H), (−L−W−H) in two dilutions (factor 10^{-1}) to identify growth of single yeast colonies. Representative image of three experiments with the same result. Successful yeast transformation was confirmed with selective medium (amino acid mix without leucine (L) and tryptophan (W) (−L−W). Dropout was performed on one −L−W and one −L−W−H plate and images were cropped during figure preparation for better visibility. Original images can be found in Figure S4. (b) Representative images of barley epidermis cells measured in FRET-FLIM showing false colour representation of meGFP lifetime as indicated by the colour bar at the bottom. Images were saved from PicoQuant SymPhoTime 64 software after lifetime fitting. (c) meGFP-tagged *Hv*GEF14 full length interacts with mCherry-tagged *Hv*RACB WT, G15V, and D121N but not with T20N RACB in FRET-FLIM experiments of barley epidermis cells. Mean GFP lifetime is indicated with orange bars and *n* = total number of cells observed in three independent experiments. Kruskal–Wallis *p* value = 4.3e−14, pairwise comparison was performed via Wilcoxon test and Bonferroni adjustment for multiple testing (Rstudio, v. 1.2.5033).

*Hv*CRIB46-mCherry (2.57 ns on average). This probably reflects the ability of WT *Hv*RACB to switch between GDP- and GTP-loaded forms also in *N. benthamiana*. As a positive control, the interaction of meGFP-CA *Hv*RACB-G15V with *Hv*CRIB46-mCherry was measured at 2.35 ns on average (Figure 5d). When additionally co-expressing HA-*Hv*GEF14 with meGFP-*Hv*RACB WT and *Hv*CRIB46-mCherry, we measured a significant decrease in meGFP fluorescence lifetime, suggesting enhanced abundance of activated CRIB46-binding *Hv*RACB-GTP. HA-*Hv*GEF14 protein stability was verified via western blot after FRET-FLIM measurements (Figure S8). Together, this

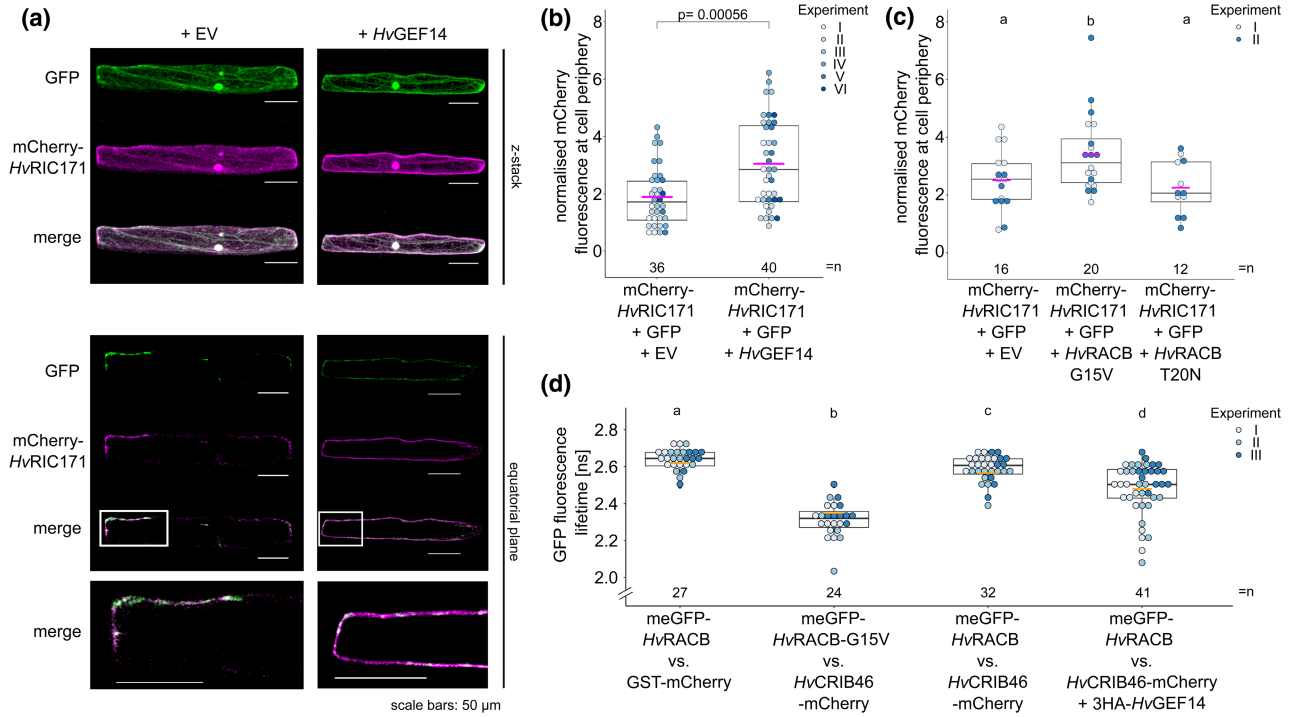

FIGURE 5 *Hv*RACB can be activated by *Hv*GEF14. The downstream interactor of activated ROPs in barley, mCherry-*Hv*RIC171, is recruited to the cell periphery when *Hv*GEF14 is co-expressed. (a) Representative images of three biological replicates show *z*-stack and equatorial plane of mCherry-*Hv*RIC171 and cytosolic GFP fluorescence of transiently transformed barley epidermis cells. (b, c) Quantification of periphery mCherry fluorescence intensity normalized to whole cell mCherry and GFP fluorescence intensity measured via Fiji. Statistical analysis performed in Rstudio via Kruskal–Wallis after testing for distribution of data (Rstudio v. 1.2.5033). (d) meGFP-*Hv*RACB interacts with *Hv*CRIB46-mCherry, a 46 amino acid fragment of *Hv*RIC171, when mutated (G15V) to a constitutively activated variant or in the presence of *Hv*GEF14 during FRET-FLIM measurements in *Nicotiana benthamiana*. GST-mCherry used as negative control. Summary of three independent repetitions indicated in shades of blue. Kruskal–Wallis comparison of means performed in Rstudio (v. 1.2.5033) after testing for distribution of data.

supports that *Hv*GEF14 can facilitate *Hv*RACB to switch into the GTP-bound signalling-activated conformation in planta.

2.5 | *Hv*GEF14 supports barley susceptibility towards penetration by Bgh

Because *HvGEF14* is expressed in barley leaf epidermal cells and *Hv*GEF14 interacts directly with *Hv*RACB, we tested the potential involvement of this exchange factor in the interaction of barley with Bgh. After transient single cell overexpression or RNAi-mediated silencing of *HvGEF14* in barley epidermis cells and subsequent inoculation with fungal spores, we scored the penetration efficiency for each transformed and attacked cell in at least five independent experiments. Every experiment represents a mean score of at least 50 observed plant–fungus interactions. On average, we observed a significant increase of successful fungal penetration from 34.6% to 46.5% (relative increase of 34%) in *Hv*GEF14 overexpressing cells when compared to an empty vector control (Figure 6). We assessed the efficacy of RNAi-mediated gene silencing to 53% by measuring the reduction of GFP fluorescence intensities of single GFP-*Hv*GEF14 expressing barley cells co-transformed with empty vector or the RNAi silencing construct (Table S4). The knockdown of *HvGEF14* by RNAi then led to the opposite effect of overexpression: a decrease in penetration rate from 26.4% in the controls to only 16.5% in cells in which *HvGEF14* was silenced by RNAi (relative decrease of 38%). Absolute penetration rates are lower in RNAi experiments due to the longer incubation time of used leaf segments after transformation. In addition, the results considerably varied from experiment to experiment, even in the controls. Accordingly, a *p* value of 0.07 was computed during statistical analysis of the means and supports a trend towards higher resistance after silencing *HvGEF14* (Figure 6). Genetic evidence thus suggests that *Hv*GEF14 supports the susceptibility of barley epidermal cells to penetration by Bgh.

3 | DISCUSSION

The barley susceptibility factor *Hv*RACB has been studied to understand molecular mechanisms of its role in supporting fungal entry into barley epidermal cells (Engelhardt et al., 2020). The transition from a GDP-bound towards the GTP-loaded signalling activated state of *Hv*RACB is probably important in this context. As shown in the model species *A. thaliana* and *O. sativa*, PRONE-GEFs can

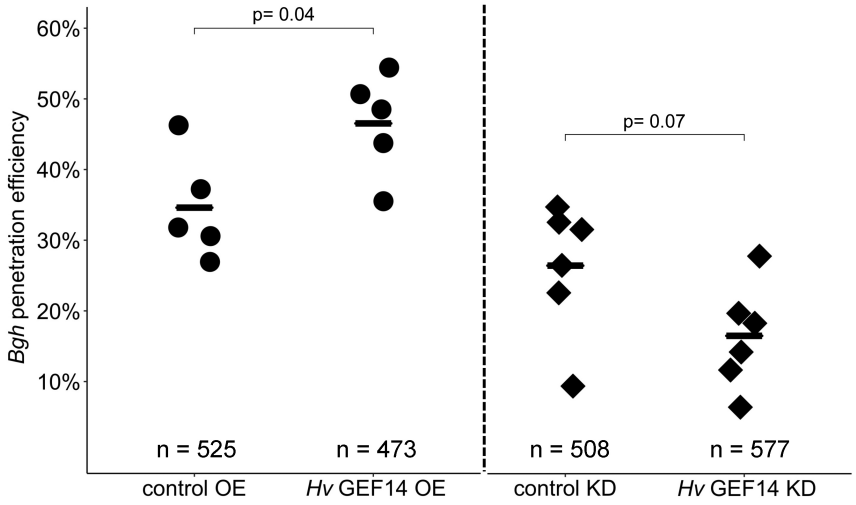

FIGURE 6 *Hv*GEF14 affects *Blumeria graminis* f. sp. *hordei* (Bgh) penetration efficiency. Bgh penetration efficiency in barley epidermis cells overexpressing (OE) *Hv*GEF14 full length compared to mean penetration efficiency in cells with pGY1 empty vector (control OE) or after knockdown (KD) of *HvGEF14* via RNAi compared to mean penetration efficiency of pIPKTA30N empty vector (control KD). Data points each show penetration efficiency of a minimum of 50 plant–fungus interactions. The mean values of all experiments are indicated with bars. Statistical significance of differences of the mean calculated with the *t* test in Rstudio (v. 1.2.5033) after assessing for normal distribution with the Shapiro–Wilk test.

facilitate the activation of ROPs. In this work, we therefore investigated the role of a barley PRONE-GEF candidate. We show the role of epidermis-expressed and transcriptionally Bgh-regulated *Hv*GEF14 in ROP activation and susceptibility to fungal penetration (Figure 7).

According to our phylogenetic analysis, we suggest that PRONE-GEF14 has a unique position in the evolution of PRONE-GEFs. A BLAST search with the primary sequence of *At*GEF14 reveals that the closest homologue to PRONE-GEF14 in the moss *Physcomitrium patens* is *Pp*GEF1 but there is no PRONE-GEF14 found in the moss (Eklund et al., 2010). In addition, in the liverwort *Marchantia polymorpha*, only one PRONE-GEF can be found in the genome. The primary sequence of this PRONE-GEF, KARAPPO, is also most similar to *At*GEF1 (Figure S6 and Hiwatashi et al., 2019). However, the ancient angiosperm species *Amborella* seems to encode a GEF14 orthologue (protein accession XP_006878646). Hence, PRONE-GEF14 proteins might have evolved early in angiosperms before separation of monocots and dicots. A unique position of GEF14 proteins in the phylogeny of PRONE-GEFs is further supported by its comparatively low sequence conservation of the PRONE domain when compared to all other PRONE-GEFs (Figure S2). Due to high confidence bootstrap analysis and comprehensive annotation of *O. sativa* and *H. vulgare* PRONE-GEFs, we propose to base future comparisons of angiosperm PRONE-GEFs on the presented phylogeny (Figure 1).

The *HvGEF14* transcript level was higher in epidermal peels when compared to whole leaves, suggesting a specific function in epidermal cells. Possible candidate ROPs to interact with *Hv*GEF14 are the epidermal cell-expressed small GTPases *Hv*RACB, *Hv*RACD, *Hv*RAC1, *Hv*RAC3, and *Hv*ROP6. When barley leaves were challenged with Bgh, several susceptibility-related barley *ROPs* had slightly lower transcript levels compared to noninoculated controls (Schultheiss et al., 2003). This gene expression profile in the epidermis is reminiscent of the *HvGEF14* expression in barley epidermis during Bgh attack (Figure 3). The powdery mildew effector Bgh-ROP-interactive peptide 1 can interact with *Hv*RACB and supports fungal virulence (Nottensteiner et al., 2018). We speculate that downregulation of *HvGEF14* transcripts and some barley *ROPs* could reflect a plant response to fungal interference with host ROP signalling, to which the plant reacts by countermeasures and downregulation of the susceptibility pathway.

GEFs are supposed to interact with signalling-inactive GDP-loaded ROP versions. This study, however, did not show direct protein–protein interaction of *Hv*GEF14 with GDP-bound dominant-negative DN *Hv*RACB-T20N in vitro or in vivo, but with WT *Hv*RACB and CA *Hv*RACB-G15V (Figure 4). The interaction of PRONE-GEFs with CA ROPs is not unheard of, however, as previous studies have shown. For instance, *Os*GEF1 interaction with *Os*RAC1 mutants was shown via split-Venus fluorescence complementation assays in protoplasts. Both the constitutively activated *Os*RAC1-G19V as well as the dominant negative *Os*RAC1-T24N variants were able to reconstitute Venus fluorescence at the plasma membrane (Akamatsu et al., 2013). Additionally, similar to studies in *A. thaliana*, which have previously shown an interaction of PRONE-GEFs with D121N-like low nucleotide affinity mutants of *At*ROPs (Akamatsu et al., 2013; Berken et al., 2005; Denninger et al., 2019; Gu et al., 2006), we observed an interaction of *Hv*RACB-D121N with *Hv*GEF14 in yeast but not consistently in planta. The initial discovery of the *A. thaliana* PRONE-GEFs was made in a Y2H screen using *At*ROP4-D121N (Berken et al., 2005) and a similar strategy was used to find PRONE-GEFs as activators of *Os*RAC1 (Akamatsu et al., 2013). Furthermore, a global investigation into *At*GEF–*At*ROP1 interactions showed that *At*GEF14

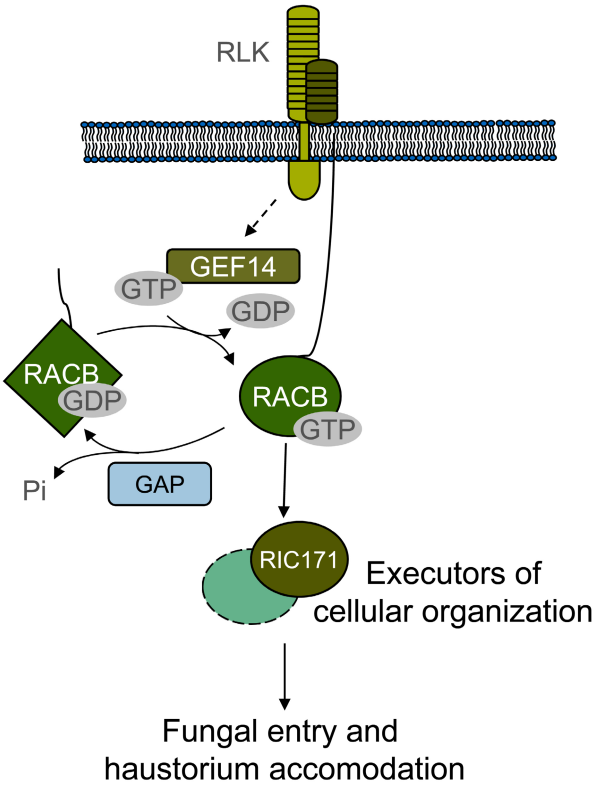

FIGURE 7 Scheme of hypothetical *Hv*RACB-dependent signalling. *Hv*GEF14 is a novel PRONE-GEF facilitating the exchange of GDP to GTP bound to the susceptibility factor and small GTPase *Hv*RACB. The membrane-associated *Hv*RACB-GTP interacts with downstream executors, such as *Hv*RIC171, to initiate changes in cellular organization that lead to fungal haustorium accommodation. GAPs (GTPase activating proteins) support GTP hydrolysis to GDP and inorganic phosphate (Pi), thereby switching off *Hv*RACB. Possible interactions between unknown receptor-like kinases (RLKs) and *Hv*GEF14 are indicated with a dashed arrow. Fungal virulence effectors and guanine nucleotide dissociation inhibitors (GDIs) are not depicted. Adapted from Engelhardt et al. (2020).

preferably interacts with a D121A/C188S mutant of *At*ROP1 in vitro (Gu et al., 2006). The D121N mutation might lead to a similar protein conformation as the nucleotide-free ROP, which has been crystallized in complex with the PRONE domain of *At*GEF8 (Thomas et al., 2007). Together, a picture emerges supporting that the GEF–ROP interaction is most stable in an intermediate, non-nucleotide-bound state. Consequently, with regard to DN *Hv*RACB-T20N, its conformation and high affinity to GDP might prevent completely the initial ROP-GEF interaction phase, which is usually quickly followed by GDP release. By contrast, activated ROPs might stay in contact with GEFs for ROP activity feedback regulation through complexes formed with ROP executers, as discussed before (Wu & Lew, 2013). Because PRONE-GEFs including *Hv*GEF14 can form dimers, GEF-GEF-ROP(GTP) interaction could also recruit further ROP-GDP for activation and therefore create a positive feedback loop to form nanodomains of ROP activity (Smokvarska et al., 2021).

Subcellular localization of signalling protein complexes is vital to ROP-mediated processes. On activation ROPs relocate to, or are stabilized in their association with, the plasma membrane. There, they interact with downstream effectors/executers to facilitate, amongst other functions, polar growth processes (Kawano et al., 2014; Poraty-Gavra et al., 2013; Schultheiss et al., 2003). During *A. thaliana* pollen tube growth, for example, the localization of activated *At*ROP1 to the apical plasma membrane regulates tip growth (Gu et al., 2004). This specific localization of activated *At*ROP1 to the membrane leads to the accumulation of downstream executers like *At*RIC4 in the same compartment. In the presence of dominant negative *At*ROP1, however, the RIC protein localizes to the cytoplasm (Gu et al., 2005). In addition, the co-expression of a ROP–GAP, which renders *At*ROP1 inactive, also results in the relocation of *At*RIC4 to the cytoplasm. The correct localization of activated *At*ROP1 as well as *At*RIC4 was observed to be crucial for downstream signal transduction and fine-tuning of the growth process (Hwang et al., 2005). To assess *Hv*RACB signalling activity status in planta, we made use of the previously published recruitment of *Hv*RIC171 by CA *Hv*RACB-G15V to the cell periphery (Schultheiss et al., 2008). We measured higher mCherry-*Hv*RIC171 localization at the cell periphery in the presence of transiently overexpressed *Hv*GEF14 (Figure 5). This suggests that the overexpression of *Hv*GEF14 leads to a higher ratio of activated endogenous ROPs, which in turn recruit *Hv*RIC171 towards the cell periphery. Our observation could even indicate that *Hv*GEF14 functions in the specific susceptibility pathway of *Hv*RIC171 in the interaction with Bgh because *Hv*RIC171 can also support fungal invasion into epidermal cells (Schultheiss et al., 2008). In this way, *Hv*GEF14 might activate *Hv*RACB, which then associates with the cell periphery to where it recruits *Hv*RIC171. In the case of a fungal attack, this localization of activated *Hv*RACB and *Hv*RIC171 was observed in context of successful fungal penetration (Engelhardt et al., 2021; Schultheiss et al., 2003, 2008). Interestingly, CA RACB-G15V likewise recruits MICROTUBULE-ASSOCIATED ROP GTPASE ACTIVATING PROTEIN1 (MAGAP1) to the cell periphery and MAGAP1 partially accumulates at the cell periphery or haustorial neck when Bgh successfully penetrates (Hoefle et al., 2011). Hence, interaction of activated *Hv*RACB with the negative regulator *Hv*MAGAP1 or other ROP GTPase activating proteins might lead to hydrolysis of RACB-bound GTP and limit the efficiency of GEF14 in inducing susceptibility towards Bgh (Figure 7).

A more direct way to measure ROP activation in planta is via CRIB-based ROP activity sensors that have previously been adapted for plants (Kawano et al., 2010; Wang et al., 2018; Wong et al., 2018). The so-called Ras and interacting chimeric unit (Raichu) sensor includes the fluorophores Venus and CFP as FRET-pair. ROP activity is monitored by its interaction with the CRIB domain of a downstream executer. In a similar manner, we used the interaction of *Hv*RACB with the CRIB domain of *Hv*RIC171 in FRET-FLIM assays (Denay et al., 2019). We observed a stronger interaction of *Hv*RACB and *Hv*CRIB46 when we co-expressed *Hv*GEF14, which strongly suggests that *Hv*GEF14 can activate *Hv*RACB in planta (Figure 5d). Additionally, transient overexpression of *Hv*GEF14 in barley epidermal cells led to

a significant increase in Bgh penetration success with 34% higher relative penetration events on average when compared to controls (Figure 6). This is comparable to enhanced fungal penetration during overexpression of CA *Hv*RACB-G15V (Schultheiss et al., 2003), as well as the overexpression of *Hv*RACB-downstream executers such as *Hv*RIC171 (Schultheiss et al., 2008) and *Hv*RIPb (McCollum et al., 2020). Transient silencing of *HvGEF14*, on the other hand, rendered barley epidermis cells on average 38% more resistant to Bgh penetration (Figure 6). Even though this effect could be observed in every repetition when comparing *HvGEF14* RNAi with its respective control, the extent of fungal penetration varied amongst repetitions so that a *p* value of 0.05 was not met after statistical analysis. Considering, however, that inoculation with Bgh naturally decreases the transcription of *HvGEF14* (Figure 3), additional ectopic knockdown perhaps cannot be expected to exert a major additional effect. Taken together, these assays point to a role of *Hv*GEF14 in supporting the accommodation of Bgh infection structures in barley epidermal cells, similar to and possibly in cooperation with the susceptibility factor *Hv*RACB and other epidermis-expressed *Hv*ROPs.

In conclusion, *Hv*GEF14 is a bona fide barley PRONE-GEF that interacts with barley ROPs. The interaction with susceptibility-related barley ROPs might lead to ROP activation and therefore facilitate ROP functions in susceptibility to invasion by Bgh. Research on *A. thaliana* PRONE-GEFs has highlighted the interplay of different PRONE-GEFs in polar growth processes like root hair formation or pollen tube growth (Denninger et al., 2019; Li et al., 2020). It remains to be studied if *Hv*GEF14 function is choreographed in a similar manner to other barley PRONE-GEFs. In addition, other PRONE-GEF interactors, such as potential upstream RLKs, remain to be investigated (Figure 7). In future studies, susceptibility- and *Hv*RACB-related candidate RLKs (Douchkov et al., 2014; Schnepf et al., 2018) will be of interest to link *Hv*RACB signalling to cell surface signal perception. *Hv*GEF14 could hence provide a link between *Hv*RACB and cell surface RLKs, and further help understanding the ROP signalling pathway co-opted by Bgh in susceptible barley.

4 | EXPERIMENTAL PROCEDURES

4.1 | Plant and pathogen propagation and maintenance

H. vulgare 'Golden Promise' was grown at 20°C, 50% humidity, and 16 h light, 8 h dark cycles for 7–8 days in standard potting soil. Bgh was propagated for 7–21 days on Golden Promise in a climate chamber at 18°C and 65% humidity, with 16 h light, 8 h dark cycles.

4.2 | Cloning procedures

Open reading frames (ORFs) of Golden Promise genes were amplified from leaf cDNA with primers (Table S5) designed on the Barley Genome (The International Barley Genome Sequencing Consortium, 2012). Constructs were cloned into Gateway destination vectors (Table S6) using BP and LR clonase (Invitrogen). Plasmids were prepared via column purification (Machery Nagel).

Binary *Agrobacterium* vectors for transformation in *N. benthamiana* and subsequent FRET-FLIM measurements were cloned using a combination of GoldenGate (Engler et al., 2008) and Gateway (Invitrogen) cloning (Table S5). Fusion constructs consisting of a fluorescent protein, a 10× glycine linker, and a protein-of-interest were first linked through *Esp*3I-mediated GoldenGate cloning and subsequently transferred into Gateway vectors through flanking *attB*sites. The necessary *Esp*3I sites and *attB*sites were introduced via overhang-PCR. Purified amplicons were assembled through *Esp*3I- and T4 DNA ligase-mediated restriction-ligation cloning (Engler et al., 2008). pDONR223 Gateway entry clones were used for transformation of *Escherichia coli* DH5α. The correct assembly of fusion constructs and integrity of sequences was confirmed via restriction digestion followed by Sanger sequencing. Subsequently, the constructs were shuffled from pDONR223 into the Gateway binary vector pGWB2 (Nakagawa et al., 2007) using Gateway LR reactions. These pGWB2 clones were used for transformation of *E. coli* DH5α. The integrity of sequences was again confirmed via restriction digestion and Sanger sequencing.

4.3 | Sequence alignment and phylogenetic tree construction

MUSCLE alignment of 14 *A. thaliana*, 11 *O. sativa* (sequences downloaded from TAIR and NCBI on 10.05.2021), and 11 *H. vulgare* PRONE-GEFs (MOREX genome v. 3) was performed in SeaView software. A maximum-likelihood (PhyML) analysis was performed with an LG model, bootstraps with 100 replicate, model-given amino acid equilibrium frequencies, nearest neighbour interchange tree searching, and five random starts. The resulting TBE tree's design was further adjusted in InkScape.

4.4 | RNA extraction and cDNA synthesis

Seven-day-old *H. vulgare* 'Golden Promise' was collected in three biological replicates. Whole-leaf and epidermal peels were cut and frozen in liquid nitrogen. Leaf tissue was ground in a tissue lyser with glass beads. RNA was extracted with TRIzol according to the protocol in Chomczynski and Sachhi (1987) and DNase I digestion was performed. Subsequently, cDNA synthesis was performed from 1 μg RNA with the QuantiTect reverse transcription kit (Qiagen) according to the supplier's protocol. cDNA from 1 μg RNA was diluted 1/10 for further analysis.

4.5 | RT-qPCR

Appropriate primers (Table S5) were used in 10 μl reactions with the Maxima 2 × SYBR Green/ROX qPCR Master Mix (Thermo Scientific)

and RT-qPCR was run on Aria Mx3000 (Agilent) with 40 cycles at 60°C for 10 s followed by 72°C for 15 s and a subsequent melting curve (65–95°C). *HvUbiquitin* was measured as a housekeeping gene (Schnepf et al., 2018) and foldchanges were calculated via the $2^{-\Delta\Delta Ct}$ method by Livak and Schmittgen (2001).

4.6 | Y2H assay

Protein–protein interactions were performed as described in the Matchmaker protocol (Clontech). *Hv*RACB (amino acids 1–193) ORF was cloned with a premature stop codon to express a truncated ROP protein lacking its C-terminal prenylation signal. *Saccharomyces cerevisiae* AH109 was transformed with pGBKT7 and pGADT7 plasmids (Table S6) containing the specific gene of interest and cultivated for 3–6 days at 30°C on synthetic dropout medium lacking amino acids leucine and tryptophan (SD−L−W). Five millilitres of liquid SD−L−W medium was inoculated with yeast colonies and on overnight cultivation at 30°C dilutions were dropped on SD−L−W and SD−L−W−H (SD lacking amino acids leucine, tryptophan, histidine) or SD−L−W−H−Ade (SD lacking amino acids leucine, tryptophan, histidine, and nucleotide adenosine) plates and incubated at 30°C.

4.7 | Protein extraction from yeast and *N. benthamiana*

Transformed yeast was cultured in 4 ml of SD−L−W overnight and centrifuged at 4000 × *g* for 5 min at 4°C. Cells were washed in 100 µl of 2 M LiAc and subsequently incubated for 5 min at room temperature in 100 µl of 0.4 M NaOH. Pellets were collected and 50 µl of 4× SDS-sample buffer was added. After vortexing, samples were boiled at 95°C for 5 min and briefly spun down before loading onto an SDS-polyacrylamide gel (Zhang et al., 2011).

Leaf discs (12 mm tissue punch) were collected from *A. tumefaciens*-transformed *N. benthamiana* leaves 48 h posttransformation and directly frozen in liquid nitrogen. Material was homogenized in a tissue lyser with glass beads and 200 µl of 4× SDS sample buffer was added. After vortexing, samples were boiled at 95°C for 10 min and spun down before loading onto an SDS-polyacrylamide gel.

4.8 | SDS-PAGE and western blot

Extracted proteins were separated by electrophoresis in a 12% polyacrylamide gel and blotted onto polyvinylidene difluoride (PVDF) membrane via semidry western blotting (protein extracted from yeast) or wet western blotting (protein extracted from *N. benthamiana*). The membrane was blocked with 5% milk in phosphate-buffered saline and incubated with specific antibodies. Proteins were detected by chemiluminescence with SuperSignal West Dura or FEMTO chemiluminescence substrate (Thermo Scientific).

4.9 | Transient biolistic transformation of barley epidermal cells

Barley cv. Golden Promise 7-day-old detached leaves were transformed by particle bombardment as described previously (McCollum et al., 2020). Two micrograms of plasmid/transformation was used in FRET-FLIM experiments. For fungal penetration efficiency experiments, 1 µg of plasmid/transformation for the gene of interest and 0.5 µg of plasmid/transformation of transformation marker (pUbi_GUSplus, β-glucuronidase) were applied.

4.10 | *A. tumefaciens* transfection of *N. benthamiana* leaves

Agrobacterium. tumefaciens GV3101 carrying binary expression vectors pGWB containing meGFP-*Hv*RACB WT, meGFP-*Hv*RACB G15V (CA), GST-mCherry, *Hv*CRIB46-mCherry, or 3xHA-*Hv*GEF14 were infiltrated into *N. benthamiana* leaves according to Yang et al. (2000). Bacterial liquid cultures were grown to OD_{600} 0.5 and mixed in equal amounts including P19 silencing suppressor. Forty-eight hours after infiltration, FRET-FLIM measurements were performed and fluo proteins were extracted for western blotting.

4.11 | FRET-FLIM

*Hv*GEF14 was N-terminally tagged with monomeric eGFP as donor and N-terminal fusions with mCherry of *Hv*RACB variants were used as acceptors. To test *Hv*RACB activation status in planta, binary vectors of meGFP-*Hv*RACB WT or meGFP-*Hv*RACB CA were co-expressed with GST-mCherry or *Hv*CRIB46-mCherry with or without co-expression of 3HA-*Hv*GEF14 via *A. tumefaciens* infiltration in *N. benthamiana* leaves.

Microscopy of transiently transformed *H. vulgare* epidermis cells and *A. tumefaciens*-infiltrated *N. benthamiana* leaf discs was performed with an Olympus FV 3000 microscope with 488 nm (20 mW) and 561 nm (50 mW) diode lasers. GFP photons were excited with a 485 nm (LDH-D-C-485) pulsed diode laser and time-correlated single photon counting (TCSPC) was performed with 2× PMA Hybrid 40 photon counting detectors. A minimum of 1000 photon counts was collected and subsequently analysed with the PicoQuant SymPhoTime 64 software. N-exponential reconvolution and decay curve fitting with daily measured or calculated IRF, for *H. vulgare* and *N. benthamiana*, respectively, was applied to gain a fit with χ^2 values between 0.9 and 1.2.

4.12 | Confocal microscopy

Transiently transformed barley epidermis cells were imaged 24 h posttransformation (hpt) with a Leica TCS SP5 confocal microscope

with hybrid HyD detectors. mCherry fluorophores were excited with a 561 nm laser and detected at 570–610 nm. GFP fluorescence was excited with a 488 nm argon laser and detected at 500–550 nm.

4.13 | RNAi efficiency

GFP-*Hv*GEF14 was transiently overexpressed together with cytosolic mCherry as a transformation marker. In addition, the empty vector of a *HvGEF14* RNAi hairpin construct of amino acids 201–401 was cotransformed and the fluorescence intensity of GFP and mCherry was measured in the *z*-stack of confocal images taken 48 hpt. RNAi efficiency was determined by the ratio of mean mCherry-normalized GFP fluorescence in *HvGEF14*-silenced cells divided by mCherry-normalized GFP-*Hv*GEF14-expressing control cells.

4.14 | Fungal penetration efficiency

Barley leaves were fixed on 0.8% water agar and inoculated 24 h after transient transformation with overexpression constructs or 48 h after transient transformation with RNAi constructs with 100 Bgh conidiospores per mm^2. Inoculated leaves were incubated for 48 h in a climate chamber at 18–22°C and 16 h light, 8 h dark. Inoculated leaves were stained in 5-bromo-4-chloro-3-indolyl β-D-glucuronic acid (X-Gluc) solution 48 h after inoculation and fixed in 80% ethanol. Fungal penetration efficiency was determined with light microscopy as described before (Hückelhoven et al., 2003).

4.15 | Statistical analysis

Statistical analyses were performed in Rstudio. Global comparison for nonparametric data was assessed with the Kruskal test and pairwise comparisons of nonparametric data were calculated via the Wilcox test with Bonferroni *p* value adjustment. Outlier tests were performed using the Grubbs test. Figures were prepared with RStudio's ggplot2 package and adjusted in InkScape.

ACKNOWLEDGEMENTS

We would like to acknowledge Johanna Hofer for outstanding technical assistance as well as Carolina Galgenmüller for pilot work on barley GEFs. Thank goes to Parvinderdeep Kahlon and Lina Muñoz for critical reading of the manuscript as well as Christopher McCollum and Michaela Stegmann for intellectual input and methodological assistance (all TU Munich). We would like to thank the Center of Advanced Light Microscopy imaging centre of TUM for providing access to the FRET-FLIM system and the TUM plant technology centre for barley propagation. We are grateful to the German Research Foundation for funding this work via SFB924. Open Access funding enabled and organized by Projekt DEAL. WOA Institution: N/A Consortia Name : Projekt DEAL

CONFLICT OF INTEREST

The authors declare no conflict of interest.

DATA AVAILABILITY STATEMENT

All data generated or analysed during this study are included in this published article (and its supplementary information files). Additional datasets used and/or analysed during the current study are available from the corresponding author on request.

ORCID

Ralph Hückelhoven https://orcid.org/0000-0001-5632-5451

REFERENCES

Akamatsu, A., Wong, H.L., Fujiwara, M., Okuda, J., Nishide, K., Uno, K. et al. (2013) An OsCEBiP/OsCERK1-OsRacGEF1-OsRac1 module is an essential early component of chitin-induced rice immunity. *Cell Host and Microbe*, 13, 465–476.

Berken, A., Thomas, C. & Wittinghofer, A. (2005) A new family of RhoGEFs activates the Rop molecular switch in plants. *Nature*, 436, 1176–1180.

Bloch, D. & Yalovsky, S. (2013) Cell polarity signaling. *Current Opinion in Plant Biology*, 16, 734–742.

Chang, F., Gu, Y., Ma, H. & Yang, Z. (2013) AtPRK2 promotes ROP1 activation via RopGEFs in the control of polarized pollen tube growth. *Molecular Plant*, 6, 1187–1201.

Chen, M., Liu, H., Kong, J., Yang, Y., Zhang, N., Li, R. et al. (2011) RopGEF7 regulates PLETHORA-dependent maintenance of the root stem cell niche in Arabidopsis. *The Plant Cell*, 23, 2880–2894.

Chomczynski, P. & Sachhi, N. (1987) Single-step method of RNA isolation by acid guanidinium thiocyanate-phenol-chloroform extraction. *Analytical Biochemistry*, 162, 156–159.

Cool, R.H., Schmidt, G., Lenzen, C.U., Prinz, H., Vogt, D. & Wittinghofer, A. (1999) The Ras mutant D119N is both dominant negative and activated. *Molecular and Cellular Biology*, 19, 6297–6305.

Denay, G., Schultz, P., Hansch, S., Weidtkamp-Peters, S. & Simon, R. (2019) Over the rainbow: a practical guide for fluorescent protein selection in plant FRET experiments. *Plant Direct*, 3, e00189.

Denninger, P., Reichelt, A., Schmidt, V.A.F., Mehlhorn, D.G., Asseck, L.Y., Stanley, C.E. et al. (2019) Distinct RopGEFs successively drive polarization and outgrowth of root hairs. *Current Biology*, 29, 1854–1865.e5.

Douchkov, D., Lück, S., Johrde, A., Nowara, D., Himmelbach, A., Rajaraman, J. et al. (2014) Discovery of genes affecting resistance of barley to adapted and non-adapted powdery mildew fungi. *Genome Biology*, 15, 518.

Eklund, D.M., Svensson, E.M. & Kost, B. (2010) *Physcomitrella patens*: a model to investigate the role of RAC/ROP GTPase signalling in tip growth. *Journal of Experimental Botany*, 61, 1917–1937.

Engelhardt, S., Trutzenberg, A. & Hückelhoven, R. (2020) Regulation and functions of ROP GTPases in plant-microbe interactions. *Cell*, 9, 2016.

Engelhardt, S., Trutzenberg, A., Probst, K., Hofer, J., McCollum, C., Kopischke, M. (2021) Barley RIC157 is involved in RACB-mediated susceptibility to powdery mildew. *bioRxiv*, 848226. [preprint].

Engler, C., Kandzia, R. & Marillonnet, S. (2008) A one pot, one step, precision cloning method with high throughput capability. *PLoS One*, 3, e3647.

Fehér, A. & Lajkó, D.B. (2015) Signals fly when kinases meet Rho-of-plants (ROP) small G-proteins. *Plant Science*, 237, 93–107.

Gu, Y., Fu, Y., Dowd, P., Li, S., Vernoud, V., Gilroy, S. et al. (2005) A Rho family GTPase controls actin dynamics and tip growth via two counteracting downstream pathways in pollen tubes. *Journal of Cell Biology*, 169, 127–138.

Gu, Y., Li, S., Lord, E.M. & Yang, Z. (2006) Members of a novel class of *Arabidopsis* Rho guanine nucleotide exchange factors control rho GTPase-dependent polar growth. *The Plant Cell*, 18, 366–381.

Gu, Y., Wang, Z. & Yang, Z. (2004) ROP/RAC GTPase: an old new master regulator for plant signaling. *Current Opinion in Plant Biology*, 7, 527–536.

Hiwatashi, T., Goh, H., Yasui, Y., Koh, L.Q., Takami, H., Kajikawa, M. et al. (2019) The RopGEF KARAPPO is essential for the initiation of vegetative reproduction in *Marchantia polymorpha*. *Current Biology*, 29, 3525–3531.e7.

Hoefle, C., Huesmann, C., Schultheiss, H., Börnke, F., Hensel, G., Kumlehn, J. et al. (2011) A barley ROP GTPase ACTIVATING PROTEIN associates with microtubules and regulates entry of the barley powdery mildew fungus into leaf epidermal cells. *The Plant Cell*, 23, 2422–2439.

Huang, C., Jiao, X., Yang, L., Zhang, M., Dai, M., Wang, L. et al. (2018) ROP-GEF signal transduction is involved in AtCAP1-regulated root hair growth. *Plant Growth Regulation*, 87, 1–8.

Hückelhoven, R., Dechert, C. & Kogel, K.H. (2003) Overexpression of barley BAX inhibitor 1 induces breakdown of mlo-mediated penetration resistance to *Blumeria graminis*. *Proceedings of National Academy of Sciences of the United States of America*, 100, 5555–5560.

Hwang, J.-U., Gu, Y., Lee, Y.-J. & Yang, Z. (2005) Oscillatory ROP GTPase activation leads the oscillatory polarized growth of pollen tubes. *Molecular Biology of the Cell*, 16, 5385–5399.

Kawano, Y., Akamatsu, A., Hayashi, K., Housen, Y., Okuda, J., Yao, A. et al. (2010) Activation of a Rac GTPase by the NLR family disease resistance protein Pit plays a critical role in rice innate immunity. *Cell Host & Microbe*, 7, 362–375.

Kawano, Y., Kaneko-Kawano, T. & Shimamoto, K. (2014) Rho family GTPase-dependent immunity in plants and animals. *Frontiers in Plant Science*, 5, 522.

Li, E., Zhang, Y.-L., Shi, X., Li, H., Yuan, X., Li, S. et al. (2020) A positive feedback circuit for ROP-mediated polar growth. *Molecular Plant*, 14, 395–410.

Lin, W., Tang, W., Pan, X., Huang, A., Gao, X., Anderson, C.T., et al. (2022) *Arabidopsis* pavement cell morphogenesis requires FERONIA binding to pectin for activation of ROP GTPase signaling. *Current Biology*, 32, 497–507.

Livak, K.J. & Schmittgen, T.D. (2001) Analysis of relative gene expression data using real-time quantitative PCR and the 2(−ΔΔ *C*[T]) method. *Methods*, 25, 402–408.

Mascher, M., Wicker, T., Jenkins, J., Plott, C., Lux, T., Koh, C.S. et al. (2021) Long-read sequence assembly: a technical evaluation in barley. *The Plant Cell*, 33, 1888–19.

McCollum, C., Engelhardt, S., Weiss, L. & Hückelhoven, R. (2020) ROP INTERACTIVE PARTNER b interacts with RACB and supports fungal penetration into barley epidermal cells. *Plant Physiology*, 184, 823–836.

Mergner, J., Frejno, M., List, M., Papacek, M., Chen, X., Chaudhary, A. et al. (2020) Mass-spectrometry-based draft of the *Arabidopsis* proteome. *Nature*, 579, 409–414.

Mucha, E., Fricke, I., Schaefer, A., Wittinghofer, A. & Berken, A. (2011) Rho proteins of plants--functional cycle and regulation of cytoskeletal dynamics. *European Journal of Cell Biology*, 90, 934–943.

Nagawa, S., Xu, T. & Yang, Z. (2010) RHO GTPase in plants: conservation and invention of regulators and effectors. *Small GTPases*, 1, 78–88.

Nakagawa, T., Kurose, T., Hino, T., Tanaka, K., Kawamukai, M., Niwa, Y. et al. (2007) Development of series of gateway binary vectors, pGWBs, for realizing efficient construction of fusion genes for plant transformation. *Journal of Bioscience and Bioengineering*, 104, 34–41.

Nottensteiner, M., Zechmann, B., McCollum, C. & Huckelhoven, R. (2018) A barley powdery mildew fungus non-autonomous retrotransposon encodes a peptide that supports penetration success on barley. *Journal of Experimental Botany*, 69, 293745–293758.

Pathuri, I.P., Zellerhoff, N., Schaffrath, U., Hensel, G., Kumlehn, J., Kogel, K.-H. et al. (2008) Constitutively activated barley ROPs modulate epidermal cell size, defense reactions and interactions with fungal leaf pathogens. *Plant Cellular Reports*, 27, 1877–1887.

Poraty-Gavra, L., Zimmermann, P., Haigis, S., Bednarek, P., Hazak, O., Stelmakh, O.R. et al. (2013) The *Arabidopsis* Rho of plants GTPase AtROP6 functions in developmental and pathogen response pathways. *Plant Physiology*, 161, 1172–1188.

Qu, S., Zhang, X., Song, Y., Lin, J. & Shan, X. (2017) THESEUS1 positively modulates plant defense responses against *Botrytis cinerea* through GUANINE EXCHANGE FACTOR4 signaling. *Journal of Integrative Plant Biology*, 59, 797–804.

Schnepf, V., Vlot, A.C., Kugler, K. & Hückelhoven, R. (2018) Barley susceptibility factor RACB modulates transcript levels of signalling protein genes in compatible interaction with *Blumeria graminis* f.sp. *hordei*. *Molecular Plant Pathology*, 19, 393–404.

Schultheiss, H., Dechert, C., Kogel, K.-H. & Hückelhoven, R. (2003) Functional analysis of barley RAC/ROP G-protein family members in susceptibility to the powdery mildew fungus. *The Plant Journal*, 36, 589–601.

Schultheiss, H., Hensel, G., Imani, J., Broeders, S., Sonnewald, U., Kogel, K.-H. et al. (2005) Ectopic expression of constitutively activated RACB in barley enhances susceptibility to powdery mildew and abiotic stress. *Plant Physiology*, 139, 353–362.

Schultheiss, H., Preuss, J., Pircher, T., Eichmann, R. & Hückelhoven, R. (2008) Barley RIC171 interacts with RACB in planta and supports entry of the powdery mildew fungus. *Cellular Microbiology*, 10, 1815–1826.

Smokvarska, M., Jaillais, Y. & Martiniere, A. (2021) Function of membrane domains in Rho-of-plant signaling. *Plant Physiology*, 185, 663–681.

Tang, W., Lin, W., Zhou, X., Guo, J., Dang, X., Li, B., et al. (2022) Mechanotransduction via the pectin-FERONIA complex activates ROP6 GTPase signaling in *Arabidopsis* pavement cell morphogenesis. *Current Biology*, 32, 508–517.

The International Barley Genome Sequencing Consortium. (2012) A physical, genetic and functional sequence assembly of the barley genome. *Nature*, 491, 711–715.

Thomas, C., Fricke, I., Scrima, A., Berken, A. & Wittinghofer, A. (2007) Structural evidence for a common intermediate in small G protein-GEF reactions. *Molecular Cell*, 25, 141–149.

Thomas, C., Fricke, I., Weyand, M. & Berken, A. (2009) 3D structure of a binary ROP-PRONE complex: the final intermediate for a complete set of molecular snapshots of the RopGEF reaction. *Biological Chemistry*, 390, 427–435.

Vetter, I.R. & Wittinghofer, A. (2001) The guanine nucleotide-binding switch in three dimensions. *Science*, 294, 1299–1304.

Wang, Q., Li, Y., Ishikawa, K., Kosami, K.-I., Uno, K., Nagawa, S. et al. (2018) Resistance protein Pit interacts with the GEF OsSPK1 to activate OsRac1 and trigger rice immunity. *Proceedings of the National Academy of Sciences of the United States of America*, 115, E11551–E11560.

Winge, P., Brembu, T., Kristensen, R. & Bones, A.M. (2000) Genetic structure and evolution of RAC-GTPases in *Arabidopsis thaliana*. *Genetics*, 156, 1959–1971.

Wong, H.L., Akamatsu, A., Wang, Q., Higuchi, M., Matsuda, T., Okuda, J. et al. (2018) In vivo monitoring of plant small GTPase activation

using a Forster resonance energy transfer biosensor. *Plant Methods*, 14, 56.

Wu, C.-F. & Lew, D.J. (2013) Beyond symmetry-breaking: competition and negative feedback in GTPase regulation. *Trends in Cell Biology*, 23, 476–483.

Yalovsky, S. (2015) Protein lipid modifications and the regulation of ROP GTPase function. *Journal of Experimental Botany*, 66, 1617–1624.

Yang, Y., Li, R. & Qi, M. (2000) In vivo analysis of plant promoters and transcription factors by agroinfiltration of tobacco leaves. *The Plant Journal*, 22, 543–551.

Zhang, T., Lei, J., Yang, H., Xu, K., Wang, R. & Zhang, Z. (2011) An improved method for whole protein extraction from yeast *Saccharomyces cerevisiae*. *Yeast*, 28, 795–798.

Zheng, Z.-L. & Yang, Z. (2000) The Rop GTPase: an emerging switch in plants. *Plant Molecular Biology*, 44, 1–9.

SUPPORTING INFORMATION

Additional supporting information can be found online in the Supporting Information section at the end of this article.

How to cite this article: Trutzenberg, A., Engelhardt, S., Weiß, L. & Hückelhoven, R. (2022) Barley guanine nucleotide exchange factor *Hv*GEF14 is an activator of the susceptibility factor *Hv*RACB and supports host cell entry by *Blumeria graminis* f. sp. *hordei*. *Molecular Plant Pathology*, 23, 1524–1537. Available from: https://doi.org/10.1111/mpp.13246